ELSEVIER

Journal of Nuclear Materials 241–243 (1997) 606–611

journal of nuclear materials

Measurements of non-axisymmetric halo currents with and without 'killer' pellets during disruptions in the DIII-D tokamak

T.E. Evans [a,*], A.G. Kellman [a], D.A. Humphreys [a], M.J. Schaffer [a], P.L. Taylor [a], D.G. Whyte [b], T.C. Jernigan [c], A.W. Hyatt [a], R.L. Lee [a]

[a] *General Atomics, P.O. Box 85608, San Diego, CA 923186-9784, USA*
[b] *INRS – Energie et Materiaux, Varennes, Quebec, Canada*
[c] *Oak Ridge National Laboratory, Oak Ridge, TN, USA*

Abstract

Non-axisymmetric halo currents are always observed during disruptive instabilities in DIII-D. These halo currents appear to have a helical structure which rotates toroidally in the electron current drift direction with frequencies ranging between 200 and 400 Hz prior to and during the initial plasma current quench phase of the disruption. Sometimes the halo current rotation locks at random toroidal phase angles during the plasma current quench. The total halo current rarely exceeds 30% of the pre-disruptive plasma current (I_{po}) and peak-to-average toroidal peaking factors (TPF) are usually less than 3 during most disruptions. Neon 'killer' pellets have proven very effective in reducing both the total halo current amplitude, often by as much as 50%, and the TPF from ~ 3 to ~ 1.2.

Keywords: DIII-D; Tokamak; Disruptions; Electric potential and current

1. Introduction

Large halo currents generated during disruptive instabilities are of major concern in high current tokamak discharges [1–3]. Since these currents flow along the open field lines in the scrape-off layer (SOL) or 'halo' region, and through the vacuum vessel, they can result in large forces on plasma facing components such as divertor structures. Understanding the origin and detailed structure of halo currents is an essential prerequisite for any tokamak reactor design. Over the last few years it has become increasingly apparent that non-axisymmetric effects play an important role in the transport of energy across the plasma boundary into the divertor [4] as well as in the current flow [5] through the SOL region of the plasma. These non-axisymmetric effects have previously been observed in the DIII-D divertor heat flux [6] during the quiescent plasma phase and are accentuated during locked modes, ELMs, and disruptions [5]. While recent measurements in Alcator C-Mod [7] confirmed the existence of non-axisymmetric components in their halo currents, there appears to be significant differences in the detailed structure of the halo currents between the two machines. It would be beneficial to understand what causes these differences. Toroidal halo current asymmetries have also recently been reported on JT-60U [8].

In DIII-D, non-axisymmetric halo currents begin growing several milliseconds prior to the plasma current quench ($-\mathrm{d}I_p/\mathrm{d}t$) and continue to rapidly evolve throughout most of the $-\mathrm{d}I_p/\mathrm{d}t$ phase. Toroidally asymmetric halo currents are a common feature of DIII-D disruptions and are measured using three arrays of (graphite) tiles located in the lower divertor, connected through calibrated shunt resistors to the vacuum vessel as described in Ref. [6]. A single poloidal array is used to determine the width of the halo region and the radial distribution of the halo current as a function of time. The poloidal layout of the halo current arrays are shown schematically in Fig. 1.

In this paper we will concentrate on results from triggered vertical displacement events (VDEs) where a com-

* Corresponding author. Fax.: +1-619 455 4156.

PII S0022-3115(96)00573-9

plete set of disruption diagnostics is available for a detailed analysis. These triggered VDEs went vertically unstable after the vertical feedback control system was disabled. In addition, we have used pellets comprised of either pure neon or deuterium doped with about 2% neon to terminate triggered VDEs and to preemptively kill quiescent plasmas. These so-called 'killer' pellets have proven to be very useful for mitigating the effects of halo currents in DIII-D and may ultimately be beneficial for providing controlled reactor shutdown scenarios. Recent 'killer' pellet results from other tokamaks [9,10] have also provided significant stimulus and encouragement for this promising new concept.

2. Experimental observations and results

Single-null diverted, ITER shaped, triggered VDEs with pre-disruptive plasma currents $I_{po} = 1.5$ MA typically evolve as follows. The vertical control system is disabled at $t = t_0$ with the magnetic axis of the plasma about 0.1 m above the machine midplane. The plasma first drifts slowly downward without much change in shape (e.g., the X-point moves down toward the floor with essentially no change in the radial position or plasma volume). At $t_1 \approx t_0 + 15$ ms the magnetic axis crosses the midplane, there is a slight reduction in the plasma volume, and the edge safety factor at the 95% flux surface q_{95} has decreased by $\approx 15\%$ with no change in the core plasma current. The plasma continues to drift downward with an exponentially increasing velocity from t_1 to $t_2 \approx t_0 + 25$ ms. By $t_3 \approx t_0 + 30$ ms the X-point touches the floor and q_{95} has dropped to about 65% of its initial value. A thermal quench begins approximately 4 ms prior to t_3, with $q_{95} \approx 2.2$–2.0, dumping most of the stored plasma energy to the divertor target plates within ~ 6–7 ms. The plasma continues to move downward during this relatively slow thermal quench and q_{95} decreases to ~ 1.5. By the end of the thermal quench the plasma has move about 60 cm below the midplane of the machine. The initial I_p quench begins at $t_4 \approx t_0 + 34$ ms, after the completion of the thermal quench, and evolves slowly until $t_5 \approx t_0 + 36$ ms when the rate of the I_p quench increases substantially along with the rate at which the plasma shrinks. The halo current amplitude typically peaks at $\sim t_0 + 35.5$ ms in these triggered VDEs.

A 'killer' pellet can be safely injected at any time between t_0 and t_2. After t_2 the plasma has moved too far down to inject a pellet since it would only graze the top of the plasma and not fully ablate, allowing it to hit the inner wall. A single cylindrical pellet 2.7 mm in diameter by 2.75 mm long with $\sim 4.5 \times 10^{20}$ neon atoms is more than sufficient to terminate the plasma. Smaller, 1.8 mm diameter by 2.75 mm long, pellets consisting of either pure neon or deuterium mixed with 2% neon are also capable of rapidly terminating the plasma. Fig. 1 shows a case in which a pure 2.7 mm diameter neon pellet was injected into the slow drift phase, $t_0 + 18$ ms $= 1718$ ms, of the VDE. The four upper traces show the radial distribution of the axisymmetric halo current component (i.e., $n = 0$ component) as a function of time for halo current arrays in rows 9 through 12, as indicated schematically at the bottom of the figure. The four equilibrium plots in the center of the figure show the position and shape of the plasma at specific times throughout the termination event. Because of the shorter thermal quench with the neon pellets (i.e., < 2 ms) and an increase in the downward vertical speed of the plasma after the pellet ablates the total duration of the VDE is reduced by as much as 10 ms on some shots.

The equilibria showing the plasma position and shape between $t = 1719$ ms and $t = 1723$ ms in Fig. 1 give a relatively clear picture of how the poloidal projection of the halo current connects through the SOL from the low field side of the vessel to the high field side. Since the plasma is leaning against the DIII-D instrumented baffle plate and bias electrode (i.e., the structures seen in the lower right-hand corner of the vessel) the halo current exits this structure and is conducted to the divertor tiles located on the high field half of the vessel (i.e., rows 9–12). The toroidal halo current array directly under the X-point or limiting point of the plasma, located in row 13, does not typically collect much current during any phase of the termination event. In addition, the row 12 array has a relatively small $n = 0$ halo current component compared to the three other halo current rings located further out in the halo plasma region (i.e., rows 9, 10, and 11) which only exists for a short time between $t = 1719$ ms and $t = 1722$ ms.

The halo current arrays in rows 9, 12, and 13 are not fully instrumented as toroidal rings which means that we must make certain assumptions about the toroidal current distribution at these poloidal positions (we presently only have fully instrumented toroidal arrays in rows 10, 11, and 14). Our working assumption is that toroidal asymmetries maintain approximately the same phase between two neighboring array rings. This allows us to estimate the axisymmetric halo current in rows 9 and 12 based on the current in the single instrumented tile in these rows and the currents in the two full toroidal rings located in rows 10 and 11, respectively. This constant phase assumption was verified on a series of shots with the row 10 and 11 rings. In addition, since the poloidal current distributions typically tend to peak on either row 10 or 11, we are confident that this assumption results in a relatively small uncertainty when estimating the total current. The ring with the largest currents is typically the 45°, row 10, array. We see from the plots in the upper part of Fig. 1 that the $n = 0$ component of the halo current peaks on the row 10 ring at $t = 1722$ ms with an amplitude of about 100 kA. The poloidal distribution of the halo current observed during the 'killer' pellet shots is typically peaked further out in the halo plasma (i.e., peaked on row 10) than in non-pellet VDEs and the total halo current is usually 50% smaller with a 'killer' pellet given the same pre-VDE conditions.

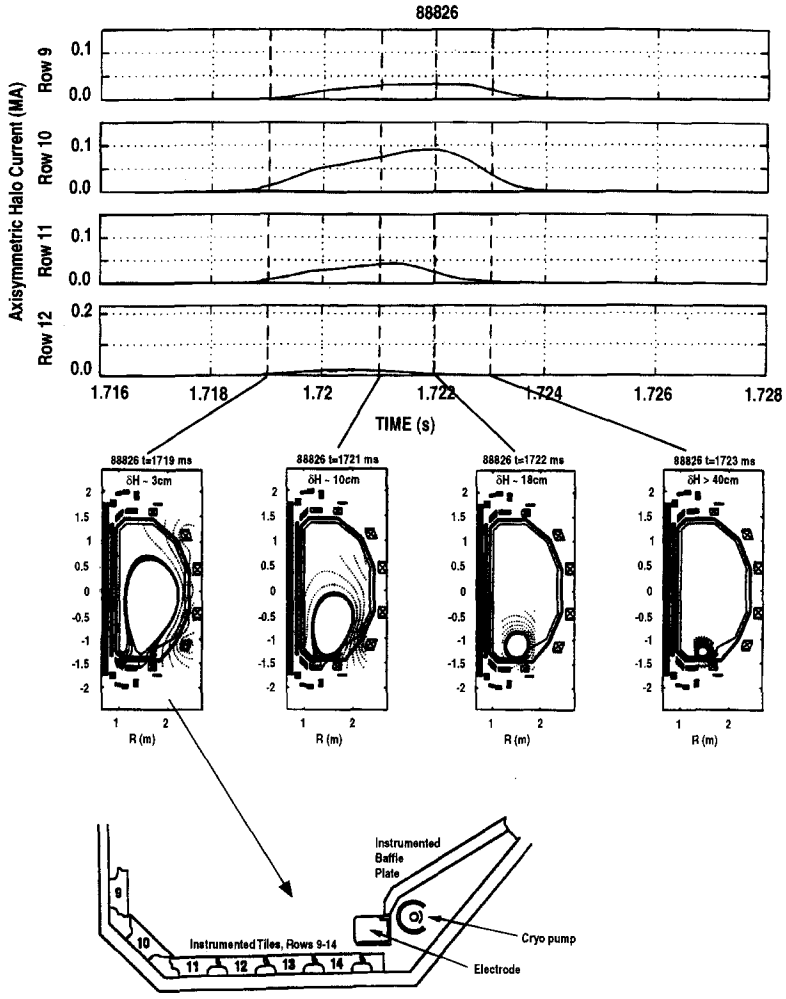

Fig. 1. Upper: the poloidal distribution of the axisymmetric component of the total halo current during a triggered VDE with a pure neon 'killer' pellet injected at $t = 1.718$ s. Center: position and shape of the magnetic flux surfaces during the evolution of the halo current. Lower: schematic layout (i.e., poloidal cross section) of the lower divertor tile current array showing row numbers referenced in the upper part of the figure.

The evolution of several important plasma parameters during a 'killer' pellet shot are shown in Fig. 2. On this shot the VDE was triggered at $t_0 = 1700$ ms and the plasma immediately began the slow downward vertical drift phase as shown in the plot of $Z(m)$. The pellet ablation light appears at $t = 1718$ ms as the pellet crosses the midplane separatrix and lasts about 0.75 ms while the pellet penetrates to $r/a \sim 0.4$. The current quench does not begin until the pellet light disappears and the plasma line density (denoted by 'Line Den R0' in Fig. 2) has increased by about a factor of 3–4 due to an abundant supply of electrons from the ablated neon. We also note a sharp spike on the central soft X-ray channel, SXR Cntr (2F12), and on the ECE (F5) signal. These signals are correlated with a spike in the hard X-ray flux indicating that a burst of runaway electrons has been lost immediately following the pellet ablation process. These runaway electrons are observed during some but not all VDEs terminated with pure neon 'killer' pellets and are never observed on VDEs without 'killer' pellets. Runaway electrons have not been seen during preemptive neon 'killer' pellet shots or VDEs terminated with 2% neon pellets.

The duration of the halo current is of order 2.6 ms (FWHM) during triggered VDEs without 'killer' pellets and about 3.0 ms during shots with neon pellets. A peak in the halo current amplitude occurs at about $0.6I_{po}$ to $0.7I_{po}$ with 'killer' pellet and at $0.8I_{po}$ to $0.9I_{po}$ during non-pellet shots. Toroidal $n = 1$ and $n = 2$ halo current components sometimes coexist and rotate toriodally in the electron current drift direction at different frequencies, although this behavior is more characteristic of 'killer' pellet shots. When this type of evolution is observed the faster mode

sometimes slows down and locks to the rotation frequency of the slower mode. Non-pellet toroidal rotation frequencies range between 200 and 400 Hz while some pellet shots rotate up to 800 Hz. Sometimes a mode makes several toroidal rotations and locks while in other cases a mode may only make a single toroidal rotation prior to locking. No preferred locking angle has been identified during these experiments. In contrast to the poloidal distribution shown in Fig. 1 for the 'killer' pellet case, a shot without a 'killer' pellet shows a broader halo current region which is fairly evenly distributed across the row 10 and 11 tiles with significantly more current on the row 12 tiles (when adjusted using the constant toroidal phase assumption discussed above). The additional halo current observed in non-pellet VDEs is confined primarily to the row 11 and 12 tiles (i.e., the inner halo plasma region).

Toroidal peaking factors (TPFs), defined as the ratio of the toroidal peak in the halo current distribution to its toroidally averaged value, of 5 are sometimes observed in the 20 kHz halo current data. Halo current data averaged with a 0.5 ms filter (which is a more relevant measure for reactor components based on their typical response time) reduces the TPF to about 3 in the worst cases. Shots without pellets have the largest TPFs at relatively low halo

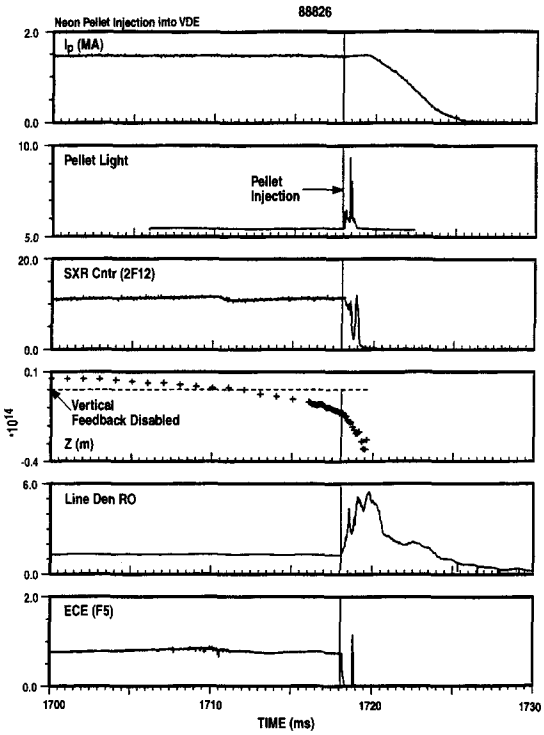

Fig. 2. Temporal evolution of the core plasma current 'I_p,' the ablation light from the neon pellet 'Pellet Light,' a central soft X-ray chord 'SRX Cntr (2F12),' the vertical position of the plasma centroid '$Z(m)$,' the line averaged plasma density 'Line Den R0,' and an electron cyclotron emission chord 'ECE (F5).'

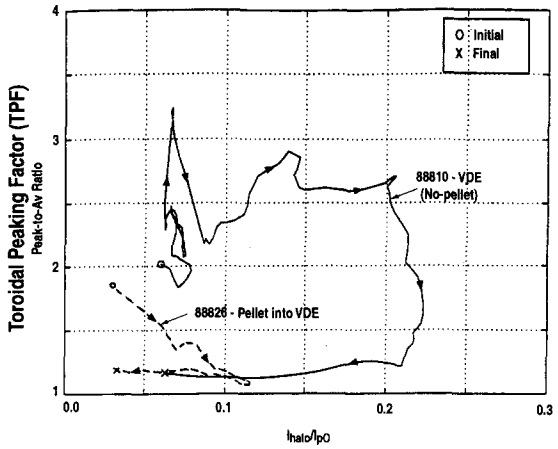

Fig. 3. The evolution of the toroidal peaking factor (TPF) peak-to-av ratio as a function of the ratio of the total halo current to the pre-disruptive core plasma current 'I_{halo}/I_{po}' for a triggered VDE without a 'killer' pellet (solid line) compared to a triggered VDE with a 'killer' pellet (dashed line).

current amplitudes. The largest TPFs occur prior to the current quench phase and the peak halo current is usually found at a minimum in the TPF. Fig. 3 shows the evolution of the TPF during VDEs with and without a neon pellet as a function of the ratio of the total halo current to the predisruptive plasma current (I_{halo}/I_{po}). The solid curve shows a non-pellet shot where the TPF fluctuates between 1.8 and 3.3 as the halo current amplitude increases (the upper part of the solid curve). As I_{halo}/I_{po} approaches ~ 0.2 the I_p quench begins and the TPF falls dramatically to ~ 1.25. By this time I_{halo} has reached a peak and the toroidal distribution of the halo current rapidly becomes very symmetric. A rapidly decaying $n = 0$ component of I_{halo} dominates most of the I_p quench phase. The dashed curve in Fig. 3 represents the TPF evolution as a function of I_{halo}/I_{po} during a neon pellet shot. Although the TPF is initially ~ 2 it rapidly decreases to below 1.2 and I_{halo}/I_{po} remains at least a factor of two less than the shot without the pellet.

Fig. 3 demonstrates how effective pure neon pellets are for reducing both I_{halo} and non-axisymmetric components of the halo current. These results were very reproducible for VDEs with $I_p = 1.5$ MA, $\beta_N = 2$, B_T of 1.5 T and 2.1 T and q_{95}s of 3 and 4. Peaks in I_{halo}/I_{po} of ~ 0.1 with both the 2.7 mm and 1.8 mm pure neon pellets (compared to ~ 0.3 in similar VDEs without pellets) are typical. TPFs of less than 1.1 are usually obtained with 2.7 mm neon pellets and TPFs of about 1.2–1.3 are obtained with the 1.8 mm pellets (compared to ~ 3.0 in similar VDEs without pellets). The TPF never exceeds 1.8 with neon pellets and is typically less than 1.2 at the peak in I_{halo}. Significant reductions in the vertical vessel motion ($\sim$ 30–40%), which is proportional to the force due to the halo current, are found during shots with pellets compared to

those without. In addition, the average I_p quench rate is reduced to $\sim 2.7 \times 10^8$ A/s with pellets compared $\sim 4 \times 10^8$ A/s without.

During one 'killer' pellet shot the timing was changed in order to inject the pellet earlier in the slow VDE drift phase. The pellet penetrated deeper into the core plasma (since the vertical position had not changed significantly) and produced an upward moving VDE rather than the usual downward event. These results suggest that the time delay between the VDE onset and the pellet arrival is important for controlling the final (fast) drift direction of the VDE. If the pellet arrives early enough during the slow drift phase (i.e., before the plasma has moved downward significantly) the plasma is forced upward. A somewhat related observation was made during preemptive plasma 'kills.' In these cases, the plasma remains relatively stationary for about 3 ms and then slowly drifts upward as it radiates most of its energy to the vessel walls. One preemptive shot with a 2% neon doped deuterium pellet appeared to remain centered on the machine midplane with no vertical motion during the entire termination event suggesting the possibility of a relatively benign soft landing with the proper mix of impurity radiation.

3. Discussion and conclusions

An important goal of the 'killer' pellet approach is to rapidly radiate away the kinetic energy of the plasma and dissipate the stored magnetic energy during the I_p quench by coupling the ohmic heating power into the strongly radiating zone. This will reduce or eliminate the heat flux conducted to the divertor plates while creating a controlled, non-disruptive, radiative shutdown of the plasma. This controlled radiative thermal quench must cool the plasma without inducing MHD instabilities which would enhance the conductive heat flow. Results on this aspect of the DIII-D 'killer' pellet work are inconclusive at this time but our experiments with neon pellets look very promising so far.

On the other hand we have conclusively demonstrated that neon 'killer' pellets are very effective in reducing the amplitude of the halo currents associated with the termination of the plasma and can essentially eliminate the non-axisymmetric components of these halo currents which are particularly dangerous in reactor scale tokamaks. In particular, large non-axisymmetric halo currents have been carefully studied during triggered VDEs in DIII-D. VDEs without 'killer' pellets typically have toroidal peaking factors (TPF) of ~ 3 with a total halo current to pre-disruptive plasma current ratio (I_{halo}/I_{po}) of ~ 0.3. Pure neon pellets and deuterium pellets doped with 2% neon are effective for reducing the TPF to ~ 1.1 and I_{halo}/I_{po} to ~ 0.1. The displacement of the vacuum vessel is also reduced with the neon 'killer' pellets and is consistent with the reduction in the halo currents which we have measured.

In addition to being non-axisymmetric, halo current generally rotate toroidally in the electron current drift direction with a frequency ranging between 200 and 400 Hz. Shots with 'killer' pellets have been observed to rotate at up to 800 Hz and have complex toroidal mode structures displaying various types of differential motion. These enhanced rotation frequencies provide an additional benefit because the vessel response to forces induced on it by the rotating halo currents is relatively slow compared to the rate of rotation of the halo current. We have also found that the toroidal rotation may persist over the entire halo current phase or may stop after a single rotation as the current locks in what appears to be a random pattern of toroidal phase angles. It is thus important to understand what determines the rate of rotation and what causes the rotation to lock. Future DIII-D killer pellet experiments will examine ways to increase the rotation frequency and prevent halo current locking.

Very short bursts, < 0.5 ms, of runaway electrons are observed on the ECE signals during the radiative thermal quench induced on some pure neon 'killer' pellets shots. These runaways are not seen during VDEs without 'killer' pellets, during preemptive pure neon 'killer' pellet shots, or during VDEs terminated with 2% neon pellets. Hard X-ray signals indicate that the runaways are not confined long enough to sustain a significant runaway electron current component. It is essential that we understand what causes these runaway electrons with some 'killer' pellets but not with others. Runaway electrons must be avoided in larger reactors such as ITER. Therefore, it is imperative that we develop and test models which allow us to scale the DIII-D results to larger tokamaks and to predict whether or not all varieties of impurity 'killer' pellets will lead to destructive levels of runaways in these machines.

Acknowledgements

The authors would like to express their gratitude to Dr. R. Khayrutdinov and the DINA Team for their simulation work in support of this project. This is a report of work supported by the U.S. Department of Energy under Contract No. DE-AC032-89ER5 1114.

References

[1] T.H. Jensen and D.G. Skinner, Phys. Fluids, B 2 (1990) 2358.
[2] J.A. Wesson, R.D. Gill and M. Hugon et al., Nucl. Fusion 29 (1989) 641.
[3] E.J. Strait, L.L. Lao, J.L. Luxon and E.E. Reis, Nucl. Fusion 31 (1991) 527.
[4] T.E. Evans, J. Neuhauser, F. Leuterer, E.R. Müller and the ASDEX Team, J. Nucl. Mater. 176–177 (1990) 202.
[5] T.E. Evans, C.J. Lasnier, D.N. Hill, A.W. Leonard, M.E.

Fenstermacher, T.W. Petrie and M.J. Schaffer, J. Nucl. Mater. 220–222 (1995) 235.
[6] D.N. Hill et al., General Atomics Report GA–Al 8908, Article 1a, July (1987) p. 5.
[7] R. Granetz et al., Nucl. Fusion 35 (1996) 545.
[8] Y. Neyatani, R. Yoshino and T. Ando, Fusion Technol. 28 (1995) 1634.
[9] G. Pautasso, O. Gruber and J.C. Fuchs et al., in: Proc. of the 22nd Euro. Conf. on Contr. Fusion and Plasma Physics, Vol. IV, Bournemouth, U.K. (European Physical Society, Petit-Lancy, Switzerland, 1995) p. 37.
[10] R. Yoshino, Y. Neyatani and N. Isei et al., in: Proc. of the 15th Inter. Conf. on Plasma Phys. and Contr. Nucl. Fusion Research 1994 (International Atomic Energy Agency, Vienna, 1995) IAEA-CN-60/A-5-II-2.